Swift Reduction of Nitroaromatics By Gold Nanoparticles Anchored On Steam-Activated Carbon Black Via Simple Preparation

Yukui Fu
Hunan University
Cui Lai
Hunan University
Wenjing Chen
Hunan University
Huan Yi
Hunan University
Xigui Liu
Hunan University
Xiuqin Huo
Hunan University
Weicheng Cao
Hunan University
Zhuotong Zeng
Central South University
Lei Qin (leiqin@hnu.edu.cn)
Hunan University

Research Article

Keywords: Carbon black, Steam activation, Au nanoparticles, Nitrophenols, Catalytic reduction

Posted Date: December 21st, 2021

DOI: https://doi.org/10.21203/rs.3.rs-1131439/v1

Version of Record: A version of this preprint was published at Environmental Science and Pollution Research on April 18th, 2022. See the published version at https://doi.org/10.1007/s11356-022-20064-w.

Abstract

Gold (Au) nanoparticles supported on certain platforms display highly efficient activity on nitroaromatics reduction. In this study, steam-activated carbon black (SCB) was used as a platform to fabricate Au/SCB catalysts via a green and simple method for 4-nitrophenol (4-NP) reduction. The obtained Au/SCB catalysts exhibit efficient catalytic performance in reduction of 4-NP (rate constant k_{app} = 2.1925 min^{-1}). The effects of SCB activated under different steam temperature, Au loading amount, pH and reaction temperature were studied. The structural advantages of SCB as a platform were analyzed by various characterizations. Especially, the result of N_2 adsorption-desorption method showed that steam activating process could bring higher surface area (from 185.9689 m^2/g to 249.0053 m^2/g), larger pore volume (from 0.073268 cm^3/g to 0.165246 cm^3/g) and more micropore for SCB when compared with initial CB, demonstrating the suitable of SCB for Au NPs anchoring, thus promoting the catalytic activity. This work contributes to the fabrication of other supported metal nanoparticle catalysts for preparing different functional nanocomposites for different applications.

1. Introduction

As raw materials for pesticides, explosives and other chemical products, nitroaromatics are widely used in the chemistry industry, which could certainly make the environmental pollution, especially water pollution, thus posing threat towards biology. For example, 4-nitrophenol (4-NP), a kind of nitroaromatics, is common toxic and in urgent need of removal (Cao et al. 2020, Fu et al. 2019a). Among the removal methods, catalytic reduction of 4-nitrophenol (4-NP) to 4-aminophenol (4-AP) is a suitable method, which can decrease the toxicity of 4-NP and simultaneously produce the added-value by-product 4-AP for many chemical synthesis and thus bring economic benefits. With abundant explorations, the catalysts for 4-NP reduction are tremendously developed in recent years, especially supported gold nanoparticles (Au NPs) catalysts (Neal et al. 2020, Zhang et al. 2020). Although the super high catalytic activity can be achieved by the supported Au NPs catalysts, the high cost and limited resource hinder the practical application (Tan &Tan 2020). Hence, it is important to design a supported Au NPs catalyst with excellent catalytic activity and desired cost.

As for catalysts supports, carbon materials with many properties of well electrical conductivity, stable mechanical performance, easy modification and low cost are widely used for Au NPs anchoring (Ferry et al. 2015, Qin et al. 2019a). In our group, we have been working on ways to develop a sequence of carbon-supported Au NPs catalysts, which are low cost and exhibit efficient catalytic performance in reduction of 4-NP (Fu et al. 2019a, Fu et al. 2019b, Qin et al. 2019a, Qin et al. 2019b, Qin et al. 2019c). For instance, we employed hierarchical porous carbon black (CB) as supporting materials to prepare supported Au NPs catalysts, on account of CB with low cost and hierarchical porous structure (Qin et al. 2019b, Wang et al. 2011). The results have shown that the rich pore structure of CB is conducive to restricting Au NPs in the pore structure, which improves the reuse ability and stability of Au NPs catalysts. In addition, the graphite-like mixed layer structure of CB can produce π-π stacking interaction, which has a strong adsorption effect on 4-NP. Compared with Au NPs catalysts supported by other carbon materials (carbon nanotubes, activated carbon and activated coke), the Au NPs supported by CB exhibits well catalytic activity (Qin et al. 2019b). In addition, to further promote the activity, stability and dispersibility of Au NPs on CB surface, N-doped and oxygen-containing groups were introduced into CB by modifying with HNO_3. The catalytic performance of the prepared bimetallic HCB-Ni-Au catalysts was certainly enhanced compared with previous study (Qin et al. 2019c). Hence, it is obvious that CB is an ideal platform for Au NPs anchoring.

The existing study has proved that CB-supported Au NPs catalysts exhibit potential for catalytic 4-NP reduction. But considering the secondary pollution to environment caused by HNO_3 modification and high toxicity of other introduced metal such as Ni, it is vital to develop an environmentally friendly method to functionalize and activate CB as a better support for Au NPs anchoring. Recently, it has been reported that steam can effectively activate carbon materials, which increases the specific area and pore volume, thus promoting the adsorption ability towards pollutants and catalytic reaction (Rajapaksha et al. 2015, Zhao et al. 2007). Lima and Huang et al. used steam to activate biomass by adjusting the temperature of steam, effectively increasing the specific area and pore volume of biomass, and the steam activated-biomass exhibited efficient adsorption ability towards Cu^{2+} and tetracycline (Lima et al. 2010, Wang et al. 2020). In the research of Shcherban et al., they also used steam to activate carbon materials (Shcherban et al. 2014). The characterization results display that the steam-activated carbon materials possess increased specific surface area and higher adsorption capacity of hydrogen. Hence, it can be expected that steam activation is a green and simple method to modify CB to increase the specific surface area and provide more active sites for Au NPs anchoring, thus promoting the catalytic activity. In addition, it has been reported by our group that ascorbic acid (AA) can serve as a mild reducing agent for Au^{3+} reduction (Fu et al. 2019b).

Thus, we expect to fabricate Au NPs supported on steam-activated CB (Au/SCB) via a green, simple and low-cost method, using AA as reducing agent. The obtained catalysts are applied in the model reaction of 4-NP reduction. The main experimental contents of this study include: (1) analysis of the characteristics of SCB compared with initial CB, and discussion the effect of steam temperature; (ii) study on the catalytic activity of Au/SCB catalysts, and discussion the effect of Au loading amount, pH, and reaction temperature, and the universality; (iii) investigation on the catalytic principle for 4-NP reduction over the Au/SCB catalysts; (iv) comparison with previous studies.

2. Experimental

2.1 Materials

Commercial spherical Vulcan XC-72 carbon black was purchased from Nanjing XFNANO Materials Technology Corporation. Hydrogen tetrachloroaurate hydrate ($HAuCl_4 \cdot 4H_2O$), ascorbic acid (AA), nitrophenols including 2-nitrophenol (2-NP), 3-nitrophenol (3-NP), 4-nitrophenol (4-NP), and 2,4-dinitrophenol (2,4-DNP), and azo dyes including Methyl orange (MO), Congo red (CR), and Erichrome Black T (EBT) were both proposed from Sinopharm Chemical Reagent Corporation Limited.

2.2 Synthesis of steam-activated carbon black supported Au NPs (Au/SCB)

Steam-activated carbon black (SCB): Commercial spherical CB was firstly purified by ultrapure water. The above samples were activated by steam for 45 min in tube furnace the peak temperature of 300°C, 400°C and 500°C with 5 $°C \cdot min^{-1}$ heating rate, and the obtained catalysts were denoted as T-SCB (T = 300°C, 400°C and 500°C).

Steam-activated carbon black supported Au NPs (Au/SCB): 0.2 g SCB was added to 100 mL of ultrapure water with ultrasound of 0.5 h. Then, 0.5~2.5 mL of $HAuCl_4 \cdot 4H_2O$ (24.28 mM) was injected into SCB suspension with stirring for 0.5 h. After that, 10 mL of AA (0.1 M) was dropwise appended into the above solution with stirring for 24 h under ambient environment. The resulting samples were collected after washed and dried overnight for further use, which were marked as xAu/T-SCB (x = 0.5, 1, 1.5, 2 and 2.5; T = 300°C, 400°C and 500°C).

2.3 Characterization

The X-Ray diffraction (XRD) was conducted on a 6100 powder diffractometer (Shimadzu Corporation, Japan). Transmission electron microscopy (TEM) was conducted on Tecnai G2 f20. Raman spectroscopy was performed on HORIBA JY LabRAM HR Evolution. Fourier transform-infrared spectroscopy (FT-IR) was collected on Perkin Elmer spectrum 100. Nitrogen adsorption isotherms were obtained by using BET surface area apparatus on Micromeritics ASAP 2460 at 423 K. X-ray photoelectron spectroscopy (XPS) was performed on apparatus of Thermo Scientific. Zeta potential was tested using a Zeta-sizer Nano-ZS (Malvern). The UV-Vis absorption spectra were monitored using UV-2700 spectrophotometer purchased from Shimadzu Corporation.

2.4 Catalytic experiments

Firstly, 10 mg xAu/T-SCB catalyst was decentralized in 50 mL 4-NP (0.2 mM), and then mixed for 30 min to realize the equilibrium of adsorption and desorption. Next, 0.0757 g $NaBH_4$ ($C_{4\text{-}NP}/C_{NaBH4}$ = 1/200) was introduced to the above solution. The solution was sampled at specific intervals time and filtrated by 0.45 μm syringe filter, and then monitored on a UV-Vis spectrometer. The catalytic reduction of various nitrophenols and azo dyes (0.3 mM) was also performed at same reaction conditions.

3. Results And Discussion

3.1 Characterizations

Firstly, XRD spectra were measured to determine the crystal structure. As shown in Fig. 1a, the typical diffraction peaks of SCB appeared at 2θ = 25° and 44° attribute to the plane (002) and (101) of carbon, which is identical with the previous results that our group reported (Qin et al. 2019b, Qin et al. 2019c). It can be initial inferred that the crystal structure of CB would not be affected by the steam. The diffraction peaks of 2Au/500°C-SCB centered at 38.1°, 44.3°, 64.5° and 77.5° can be ascribed to the plane (111), (200), (220) and (311) of face-centered cubic (fcc) Au (JCPDS No.04-0784), respectively. It can be noticed that the peak intensity attributed to plane (002) of SCB decrease in 2Au/500°C-SCB sample, which is because the Au NPs weaken the internal structure order of SCB (Qin et al. 2019b, Xia et al. 2016).

TEM and HRTEM characterizations were conducted to study the morphology and microstructure of 500°C-SCB and 2Au/500°C-SCB catalysts. As shown in Fig. 1b, it can be observed that the SCB is spherical morphology with size of ~40 nm and slightly aggregation, which is similar with the morphology of initial CB in our previous research (Qin et al. 2019b). As for the morphology of 2Au/500°C-SCB catalysts shown in Fig. 1c-e, it can be preliminary estimated that Au NPs with size of ~65 nm is well dispersed without obvious aggregation on the surface of SCB. It can be primarily attributed to the fact that CB activated by steam can provide much active sites on the surface for Au anchoring (Wang et al. 2011). HRTEM image (Fig. 1e) displays the distinct lattice fringes of 0.235 nm, ascribed to the plane (111) in fcc Au NPs, which further demonstrates that the Au NPs were resoundingly immobilized on the 500°C-SCB surface (Fu et al. 2019a). Fig. 1f displays the STEM image of 2Au/500°C-SCB catalysts. Interestingly, it can be found that except large-sized Au NPs (~65 nm) anchored on the surface of SCB, the small-sized Au NPs (~5 nm) are also anchored both inside and on the surface of SCB, which may be ascribed to plentiful hierarchical porous texture and high specific area of SCB (Qin et al. 2019c).

Next, Raman and FT-IR spectroscopy were used to provide more information on the crystallinity and surface groups of samples. As shown in Fig. 2a, two characterization peaks at 1345 cm^{-1} attributed to D band and 1560 cm^{-1} attributed to G band appear in the Raman spectra of initial CB (Reddy et al. 2020, Revathy et al. 2018). The D band indicates the disorder or defect in this lattice, and G band indicates the 'in-plane' vibrations. Usually, the ratio of I_D/I_G is used to represent the degree of disorder in the graphitic material (Revathy et al. 2018). I_D/I_G ratio of the initial CB and SCB are calculated to be 1.06 and 1.16. Obviously, the I_D/I_G ratio of SCB increases when compared with initial CB, representing more defects are brought into SCB and the graphitization degree decreases after steam activating (Song et al. 2014). As for 2Au/500°C-SCB, the I_D/I_G ratio was calculated to be 1.07, closed to the value of initial CB. It may be because the nucleation of Au NPs at SCB surfaces fills up a part of defect sites on SCB surface (Ballesteros et al. 2008). Furthermore, FT-IR spectra provide the information about surface chemistry as shown in Fig. 2b-c. All spectra of samples display a peak at 3680-3080 cm^{-1}, ascribed to water (hydroxyl groups), which can be neglected following the subsequent discussion (Fu et al. 2019a, Fu et al. 2019b). The peak at 1626 cm^{-1} is associated to C=C bonds or characteristic of condensed aromatic structures (Shcherban et al. 2014). In addition, the peaks around 1170-1000 cm^{-1} and 695-554 cm^{-1} are responsible for stretching and plane bending vibrations of C–H bonds (Fu et al. 2019a, Qin et al. 2019b). Compared with initial CB that we have test the characterization in other study, there is no characteristic band in region 2890-2350 cm^{-1} in the SCB samples activated at different temperature (300°C, 400°C, and 500°C), which may be ascribed to the steaming purification (Ballesteros et al. 2008). According to FT-IR results, no obvious change was detected for surface chemical properties after steam activating. After loading Au on SCB surface, there is no obvious change in all peaks that were located in the same position (Ali et al. 2017, Kamal et al. 2016).

The pore structures of initial CB, 500°C-SCB and 2Au/500°C-SCB were tested by N_2 adsorption-desorption method. Fig. 2c-d indicate the N_2 adsorption-desorption isotherms follow the type IV classification, indicating the existence of abundant mesopores in these samples. Table S1 lists the specific surface area on the basis of Brunauer-Emmett-Teller (BET) model. Obviously, the BET surface area of 500°C-SCB (249.01 m^2/g) is higher than that of initial CB (185.97 m^2/g), which can be ascribed to the steam activating (Rajapaksha et al. 2015). Similarly, the pore volume of 500°C-SCB also increases to 0.165 cm^3/g from 0.073 cm^3/g. Differently, the pore size of 500°C-SCB decreases to 15.61 nm when compared with initial CB (21.04 nm). Hence, pore size distribution on the basis of Barrett-Joyner-Halenda (BJH) and Horvath-Kawazoe models were used to further explain the decrease of pore size. As shown in Fig. 2d, there is a main peak within the range of mesopore diameters (10-50 nm) in the pore size distribution of initial CB, while the peak in the range of micropore diameters (0-2 nm) is appeared in 500°C-SCB, exhibiting hierarchical pore structures. All the results clearly illustrate that steam activating process can bring higher specific surface area, larger pore volume and more micropore structures (Jiang et al. 2013, Rajapaksha et al. 2015, Shcherban et al. 2014). It can be explained by that the process causes the rapid and continuous diffusion of gases, especially superheated steam, into the CB, thus exposing new surfaces and forming more micropores in SCB (Lima et al. 2010). Remarkably enough, the larger specific surface area may be owing to more pores from stacking together, and the large amount of emerged micropores result in the decreased average pore size in 500°C-SCB (Li et al. 2021). After loading Au NPs, the specific area and pore volume of 2Au/500°C-SCB display a little decrease, which may be because the Au NPs occupy a portion of surface and pore channel of 500°C-SCB, in accord with the results of TEM analysis.

To further understand the effect of steam activating on samples, XPS was performed to analyze the chemical composition and chemical bonds over the initial CB, 500°C-SCB, and 2Au/500°C-SCB. The full XPS spectra presented in Fig. 3a display the compositional elements of them, illustrating C and O elements are the dominant species in each sample. As shown in Fig. 3b, the high-resolution C 1s spectra is deconvolved into four peaks with binding energy (BE) at 284.6, 285.8, 286.9 and 289.8 eV, ascribed to sp^2 carbon (graphitic C=C), sp^3 carbon (hydrocarbon C–C), C–O and π-π transition loss (Wang et al. 2011, Xia et al. 2016). The relative

rations (%) of four species for initial CB, 500°C-SCB, and 2Au/500°C-SCB are listed in Table S2. It is obvious that the relative percentage of C=C decreases to 55.59% from 66.1%, and C–C increases to 28.35% from 9.83% after steam activating. The results are consistent with the discussion in the section of Raman analysis, that the graphitization degree decreased and more defects are brought into SCB after steam activating, owing to the etch of crystal structures by the steam activating. In addition, the relative percentage of C–O increases to 7.91% from 6.43% after steam activating. As shown in Fig. 3c, the percentage of O also increases for SCB after steam activating, corresponding to the results of increased percentage of C–O. After loading Au NPs, the high-resolution spectrum of C 1s displays that the percentage of C–O still increases to 16.81%. According to the previous reports by Xie et al., it could be associated with the improved uniformity of Au NPs on SCB because the C–O could serve as active sites with high charge density on the oxygen sites (Wang et al. 2011). The Au 4f spectrum shown in Fig. 3d displays the typical characteristic peaks at 83.2 and 86.9 eV, displaying Au $4f_{7/2}$ and Au $4f_{5/2}$ of Au^0 (the difference value between the two peaks is 3.7 eV). In addition, the additional peaks at the high BE side are also found, attributed to oxidized Au^+ species (Duan et al. 2019, Qin et al. 2021).

3.2 Catalytic performance of Au/SCB catalysts for nitrophenols reduction

3.2.1 Catalytic performance for 4-NP reduction

The reaction of 4-NP reduced to 4-AP is thermodynamically feasible (E^o = -0.76 V) at normal conditions with $NaBH_4$ serving as reductant (E^o = -1.33 V) (Zhang et al. 2021). However, the reaction progress is hard to proceed without catalyst, owing to the kinetic barrier brought from large potential difference between 4-NP and $NaBH_4$. But the barrier could be got over through Au NPs based catalysts and the reaction progress is readily detected by UV-vis spectrometer (Jiang et al. 2021). Hence, Au/SCB catalysts was used for catalytic 4-NP reduction. Firstly, adsorption experiments of 4-NP by SCB and Au/SCB catalysts were conducted. Fig. S1a-b show that the peak intensity at 316 nm of 4-NP decreases but there is no new peak in the absorbance spectra, demonstrating the adsorption ability of SCB and Au/SCB catalysts. Fig. S1c displays that the absorbance characteristic peak of 4-NP shifts from 316 to 400 nm after adding $NaBH_4$, illustrating 4-nitrophenolate ions are formed (Fu et al. 2019a, Qin et al. 2019c). When adding 2Au/500°C-SCB catalyst, the peak intensity at 400 nm slowly weakened with the reaction proceeding and could be detected no longer after 3 min, indicating the 4-NP reduction. Meanwhile, a new peak occurred at 300 nm, indicating the formation of 4-AP (Fig. 4a). In addition, the color of reactants gradually fades. The $NaBH_4$ concentration is 200 times 4-NP concentration, so the catalytic 4-NP reduction can be regarded as pseudo-first-order kinetics reaction. After simulating, the rate constant k_{app} was obtained (2.1925 min^{-1}), displaying excellent catalytic activity of 2Au/500°C-SCB catalyst (Fig. 4b).

3.2.2 Effect of steam activating temperature and Au loading amount

According to the previous study, it is known that the temperature of steam activating may impact on the structure of SCB, thereby influencing the catalytic activity of Au/SCB catalysts. Besides, the loading amount of Au is also an important parameter for the Au-based catalysts. Hence, the effects of steam activating temperature and Au loading amount were investigated. As shown in Fig. S2a-c, all the xAu/T-SCB catalysts (x = 0.5, 1, 1.5, 2 and 2.5; T = 300°C, 400°C and 500°C) can successfully reduce 4-NP (Fig. S2d-f). As evidenced in the kinetic rates, the catalytic performance of different xAu/T-SCB catalysts is closely related to the steam activating temperature and Au loading amount. Obviously, the catalytic performance is promoted as the steam activating temperature increases from 300°C to 500°C. Among the Au/SCB catalyst prepared in different temperature, the Au/500°C-SCB displays the highest catalytic activity for 4-NP reduction. It might be because that the higher temperature may be beneficial for superheated steam diffusing, resulting in high specific area and abundant pore structure, especially micropore, which is demonstrated by the BET characterization (Table S1). The abundant pore structure is conducive to concentrating 4-NP, thus facilitating the catalytic activity (He et al. 2020). As for different Au loading amount, all the catalysts with 2 mL of Au loading amount prepared under different temperature exhibits higher catalytic activity. Fig. S2d-f displayed the $-\ln(C_t/C_0)$ *vs.* time of 4-NP reduction over xAu/T-SCB catalysts (x = 0.5, 1, 1.5, 2 and 2.5; T = 300°C, 400°C and 500°C). With Au loading amount increasing, the catalytic rate is firstly increased and next decreased. It might because the active sites increased with Au content increasing, while the active sites would decreased caused by Au NPs agglomeration with Au content further adding (Jiang et al. 2021). The rate constant k_{app} is 1.4869, 2.0382 and 2.1925 min^{-1} for 2Au/300°C-SCB, 2Au/400°C-SCB and 2Au/500°C-SCB, respectively. Overall, considering the catalytic efficiency and economic cost, 2Au/500°C-SCB exhibits better performance, thus employed in the following study.

3.2.3 Effect of initial pH

The effect of pH in this catalytic system was investigated at initial pH of 2-9. As shown in Fig. 5a, it is obvious that initial pH can significantly affect the catalytic activity of 2Au/500°C-SCB and the acidic pH condition is beneficial for promoting the catalytic efficiency. With the initial pH increasing from 2 to 9, the catalytic activity decreased to 0.4022 min^{-1} from 3.8387 min^{-1} (Fig. 5b). It has been reported that the effect of pH in this catalytic system is closely associated with the pH_{IEP} of 2Au/500°C-SCB and pK_a of 4-NP (Nellaiappan et al. 2017, Nguyen et al. 2019a). Zeta potential of the 2Au/500°C-SCB was measured to better understand the influence. Fig. S3 shows the Zeta potential of 2Au/500°C-SCB, which shows a decreasing trend from positive potential to negative potential. The measured pH_{IEP} of 2Au/500°C-SCB is at about pH of 4, indicating that the catalysts are positively charged at pH < 4. It can been known that the catalytic 4-NP reduction by 2Au/500°C-SCB in the presence of excessive $NaBH_4$ conforms to Langmuir-Hinshelwood kinetics model, in which the primarily step procedure is adsorption for catalytic reduction reaction (Qin et al. 2019c). Hence, the BH_4^- with negative charge would be readily gathered round the 2Au/500°C-SCB surface with positive charge at acidic condition, thus leading to an improved rate constant. In addition, protons in solution can easily bond with BH_4^- to produce H_2 at acidic condition, promoting the formation of activated H and thus enhancing the catalytic activity (Lin &Doong 2014). The results are in well accord with the results obtained from the previous study of Lin and Doong et al., that low pH condition is conducive for accelerating the catalytic efficiency (Lin &Doong 2014, Nguyen et al. 2019b). When pH increases over 5, the form of 4-NP with pK_a of 7.2 is anionic. It means that 4-NP anions can be not easily adsorbed onto the negatively charged 2Au/500°C-SCB surface on account of the electrostatic repulsion, thus decreasing the catalytic efficiency (He et al. 2020). The results reflect that the adsorption process is vital for the catalytic reaction, which would be focused on following discussion about the catalytic mechanism.

3.2.4 Effect of reaction temperature

Reaction temperature on 4-NP reduction was also studied from 20°C to 60°C. Fig. 5c-d display that the catalytic rate of 4-NP reduction increased with temperature increasing, and the rate constant for 4-NP reduction increased from 0.8952 min^{-1} at 20°C to 2.7531 min^{-1} at 60°C. According to the previous study, increasing temperature can accelerate decomposition of $NaBH_4$ and generation of activated H on catalyst surface, thus enhancing the catalytic activity (Ozerova et al. 2020). Furthermore, activation energy (E_a) can reveal the relation and dependency between the temperature and rate constant in catalytic reactions (Shin et al. 2012, Wang et al. 2021), which can be evaluated based on the Arrhenius equation (Eqs. (1)).

$$\ln k = \ln A - E_a / RT \quad (1)$$

in which A and T display pre-exponential factor and temperature respectively, and R indicates gas constant (8.314 $JK^{-1}{\cdot}mol^{-1}$). As shown in Fig. S4, the linear fitting of ln k *vs.* $1/(T \times 1000^{-3})$ is obtained, in which E_a can be figured from the slope ($-E_a/R$) (Cui et al. 2020). Hence, the E_a of 2Au/500°C-SCB for reducing 4-NP is calculated as 23.235 kJ/mol. It is approximate with the E_a of other reported Au-based catalysts, indicating the well activity of 2Au/500°C-SCB for 4-NP reduction. Generally, the E_a in the range of 8–42 kJ/mol could be ascribed to surface catalyzed reactions. Hence, it can be concluded that the catalytic 4-NP reduction over 2Au/500°C-SCB fits surface catalytic mechanism (Bogireddy et al. 2020, Cao et al. 2020, Cui et al. 2020, Wang et al. 2021).

3.2.5 Catalytic activity for isomers and homologues of 4-NP

To manifest the generality of as-prepared 2Au/500°C-SCB catalysts and figure out the impacts of substituent groups, catalytic reduction of isomers of 4-NP such as 2-NP and 3-NP, homologues including 2, 4-DNP was investigated under the same reaction conditions. As shown in Fig. S5a-c, the 2Au/500°C-SCB catalysts exhibit satisfactory catalytic activity for nitrophenols. The absorbance peaks attributed to 2-NP (414 nm), 3-NP (390 nm) and 2, 4-DNP (443 nm) gradually weakened after adding 2Au/500°C-SCB catalysts (Fu et al. 2019b), and all the color of reactants faded from natural color. Fig. S5d displays that 2-NP and 3-NP can be totally reduced within 3 min, and the catalytic reduction of 2, 4-DNP is accomplished within 4 min. The different catalytic efficiency for isomers and homologues of 4-NP may be attributed to the molecular orientation and number of nitro-substituent, which has been reported in our previous study (Fu et al. 2019b).

3.2.6 Catalytic activity for azo dyes

In addition to nitrophenols, azo dyes involving azo bond (–N=N–) in wastewater could also bring serious threat to environment and human health. The catalytic reduction of –N=N– over metal NPs catalyst has proved an efficient method to cleavage –N=N– and thus reducing its hazard (Zhang et al. 2021). Hence, some typical azo dyes such as MO, CR and EBT were selected to further study the catalytic universality of 2Au/500°C-SCB catalysts. Fig. S6 shows that the peak intensity of MO (463 nm), CR (497 nm), and EBT (530

nm) decreases as the reaction proceeding with the decolorization of reaction solution, until it can be detected no longer. Simultaneously, a new peak occurred at ~250 nm, illustrating the formation of new colorless products. The new peak may be ascribed to derivatives of azo dyes after azo bonds splitting (Fu et al. 2019a). Obviously, the catalytic efficiency of MO and CR reduction was higher than that of EBT, which might because 2Au/500°C-SCB exhibits different adsorption capacity towards various azo dyes, and different azo dyes possess different structure (Qin et al. 2019c). Even so, the 2Au/500°C-SCB catalysts exhibit well catalytic activity in various azo dyes reduction.

3.2.6 Recycling stability of catalyst

As shown in Fig. S7a, the 2Au/500°C-SCB catalyst exhibits well stability with no obvious deactivation after 5 recycles experiments. But the rate constant k_{app} for nitrophenol reduction decreases when the catalysts are reused, which may be because the production of 4-AP with $-NH_2$ is bonded on the surface of Au NPs. It has been known that $-NH_2$ could strongly bind with Au NPs, therefore blocking the catalytic sites on Au NPs. To verify the assumption of surface blocking by $-NH_2$, 4-AP was used to pretreat the 2Au/500°C-SCB catalysts prior the reduction of 4-NP. Fig. S7b displays that the catalytic 4-NP reduction over the 4-AP pretreated 2Au/500°C-SCB catalysts is complete within 11 min and the rate constant k_{app} decreases to 0.3765 min^{-1} from 2.1925 min^{-1}, verifying the assumption of surface blocking by $-NH_2$.

3.3 Catalytic mechanism

The catalytic principle for 4-NP reduction over Au-based catalysts has been widely proposed and verified in previous studies. In this study, a widely feasible electron transfer principle is employed, i.e. BH_4^- as electron donors and $-NO_2$ on 4-NP as electron acceptor, which can be divided into three main stages (Bian et al. 2021, Liu et al. 2021). Firstly, BH_4^- and 4-NP were adsorbed on Au/500°C-SCB surface. Meanwhile, the adsorbed BH_4^- would dissociate and activated by BH_4^- and then active Au-H was formed. Then, active Au-H and electron transferred to 4-NP, leading to $-NO_2$ reduction to $-NH_2$. Finally, 4-AP desorbed naturally from 2Au/500°C-SCB surface (Bogireddy et al. 2020, Liu et al. 2021). Combined with the results of characterizations, the superior catalytic features of 2Au/500°C-SCB catalysts could be explained by following respects: (i) the steam activation may bring some defects to SCB for providing more active sites for Au NPs anchoring, thus forming more catalytic sites for 4-NP reduction. (ii) It has been discussed that adsorption process is vital for catalytic reaction. Compared to initial CB, the BET specific area and pore volume of SCB increase significantly, and micropore structure appeared. These are beneficial for adsorption, thus facilitating diffusion/transport of 4-NP/4-AP. (iii) In addition, the increased BET surface and porosity could lead to a significant increase of hydrogen adsorption, which is conducive to the production of active hydrogen species on Au NPs and further promotes the catalytic activity (Shcherban et al. 2014). Fig. 6 shows the process of preparing 2Au/500°C-SCB catalysts applied in 4-NP reduction, which is a green and simple method.

3.4 Comparison with previous studies

As for a catalyst used in catalytic reaction, the critical factors in practical application should possess super high activity and effective cost. Our group has been working on ways to design supported Au NPs-based catalysts with super high activity and low cost. As discussed above, the 2Au/500°C-SCB catalysts exhibit expected catalytic performance towards 4-NP reduction. Table 1 compares the obtained catalysts in this study with supported Au NPs catalyst reported by our previous studies and other recent publications. The catalytic performance is emphasized.

It should be noticed that although the 2Au/500°C-SCB catalysts is similar to the Au/CB catalysts in our previous study, in which the initial CB was used for supporting Au NPs, 2Au/500°C-SCB catalysts display different structure. The results of Nitrogen adsorption isotherms and TEM show that the pore structure of initial CB mainly composes of micropores, mesopores and macropores, which may be caused by the aggregation of dispersed CB. After anchoring Au NPs on the initial CB, the specific area, pore volume, and average pore size decreases, indicating that Au NPs are limited in the porous structure of CB. But in this study, the results of Nitrogen adsorption isotherms illustrate that the specific surface area of SCB increases to 249.0053 m^2/g, and more micropores structure appears when compared with initial CB. Combining with TEM results, it can be found that Au NPs are located inside and on the surface of SCB. In addition, the Raman structure displays that more defects are brought into SCB, providing more active sites for Au NPs anchoring. It can be reasonable speculated that steam activation brings the structure advantages to SCB for supporting Au NPs. Hence, the performance of 2Au/500°C-SCB catalysts in this study is also improved greatly. Under the same reaction condition, the catalytic reduction of 4-NP over 2Au/500°C-SCB catalysts could be finished within 3 min, while the reaction over Au/CB catalysts was complete within 5 min. The rate constant k_{app} of Au/500°C-SCB for 4-NP reduction increased to 2.1925 min^{-1}, but the rate constant k_{app} of Au/CB catalysts was

0.8302 min^{-1} (Qin et al. 2019b). The enhanced catalytic activity of 2Au/500°C-SCB catalysts could be ascribed to the steam activation, bringing more active sites for Au NPs anchoring and more hierarchical pore structure.

Although the catalytic activity of 2Au/500°C-SCB catalysts is not as good as the HCB-Ni-Au and PDA-g-C_3N_4/Au catalysts prepared in our previous studies, the modification method for CB supports is eco-friendly and easy accessibility. And the reductant AA is gentler than $N_2H_4{\cdot}H_2O$, which would not bring about secondary pollution during synthesis. Besides, compared with other catalysts such as Ag@RF@Fe_3O_4 nanocatalysts and Pt/biogenic SiO_2 hybrid, although 2Au/500°C-SCB catalysts do not exhibit better catalytic activity, the CB supports in this study are cheaper and easily available. Nevertheless, the activity of the obtained catalysts in this study should be further promoted, which is doing under our laboratory.

Table 1
Comparison of the catalytic performance of Au/500°C-SCB with our previous studies and recent published studies.

Samples	Support	Modification method for support	Synthesis method	k_{app} (min^{-1})	k_{nor}[b] ($min^{-1}{\cdot}mg^{-1}$)	m (catalyst, mg)/V (solution, mL)	Ref.
2Au/500°C-SCB	Carbon black	Steam activating CB	AA as reducing agent	2.1925	0.2192	1/5	This study
Au/CB	Carbon black	-	Ethylene glycol as reducing agent	0.8302	0.0830	1/5	(Qin et al. 2019b)
HCB-Ni-Au	Carbon black	HNO_3 modifying CB	$N_2H_4{\cdot}H_2O$ as reducing agent	1.9617	0.3923	1/10	(Qin et al. 2019c)
Au/AC	Activated coke	-	AA as reducing agent	1.1496	0.1277	3/10	(Fu et al. 2019b)
Au NPs/CTS/AC	Activated coke	Chitosan functionalized AC	Chitosan as reducing agent	0.6994	0.1399	1/10	(Fu et al. 2019a)
PDA-g-C_3N_4/Au	g-C_3N_4	Polydopamine decorated g-C_3N_4	Polydopamine as reducing agent	3.0840	0.6168	1/6	(Qin et al. 2019a)
Au/$M_{2.5}$-ZSM-5(2d)	silica ZSM-5 zeolite	-	$NaBH_4$ as reducing agent	0.3450	0.1725	2/3	(He et al. 2020)
Ag@RF@Fe_3O_4 nanocatalysts	Resorcinol formaldehyde@Fe_3O_4	Resorcinol formaldehyde	Photocatalytic reduction	2.2700	5.4900	1/10	(Cao et al. 2020)
Au@graphitic carbon nitride	graphitic carbon nitride	-	Photodeposition method	0.3198	0.1599	1/1	(Nguyen et al. 2019b)
Pt/biogenic SiO_2 hybrid	Biogenic porous silica particles	-	Impregnation method	1.7400	7.2500	1/250	(Bogireddy et al. 2020)

4. Conclusions

In this paper, we have designed a green and economic way to fabricate xAu/T-SCB catalysts using steam activated CB as supports and AA as reducing agent. By comparing the characteristics of initial CB and SCB activated by steam at different temperatures, the 500°C-SCB is more apt to serve as benign platform to anchor Au NPs. Because it has applicable defects and high BET specific surface area, which is brought by steam activation, thus providing quite active sites for Au NPs anchoring both inside and on the surface of SCB. The obtained 2Au/500°C-SCB catalysts exhibit high catalytic efficiency in 4-NP reduction with k_{app} of 2.1925 min^{-1}. The superiority of 2Au/500°C-SCB catalysts can be explained by the adequate catalytic active sites of Au NPs and competent adsorption ability for pollutants ascribed to the above properties of SCB. Furthermore, the enhanced hydrogen adsorption may also be conducive to the production of active hydrogen species on Au NPs, thus promoting the catalytic activity. In addition, the 2Au/500°C-SCB catalysts exhibit

well universality and recyclability, which is important for the industrial application. The steam activated SCB for Au NPs anchoring in this study offers a guidance for anchoring different nanoparticles to prepare functional nanocomposites, which could be used in different applications.

Declarations

Ethical Approval

Not applicable

Consent to Participate and Consent to Publish

Not applicable

Authors Contributions

Conceptualization: Yukui Fu and Cui Lai

Methodology: Wenjing Chen and Huan Yi

Formal analysis and investigation: Xigui Liu and Xiuqin Huo

Writing - original draft preparation: Yukui Fu and Lei Qin

Writing - review and editing: Weicheng Cao, Zhuotong Zeng and Lei Qin

Funding acquisition: Cui Lai, Zhuotong Zeng and Lei Qin

Supervision: Zhuotong Zeng and Lei Qin

Funding

This study was financially supported by the Program for the National Natural Science Foundation of China (82003363,82073449, U20A20323, 51521006, 51879101, 51579098, 51779090, 52100183), the National Program for Support of Top–Notch Young Professionals of China (2014), the Program for Changjiang Scholars and Innovative Research Team in University (IRT-13R17), and Hunan Natural Science Foundation (2020JJ3009), Hunan Researcher Award Program (2020RC3025), Postgraduate Scientific Research Innovation Project of Hunan Province (CX20210408), the Science and Technology Innovation Program of Hunan Province (2021RC2057), the Fundamental Research Funds for the Central Universities (531118010473), and the National Natural Science Foundation of Changsha (kq2007059).

Competing Interests

The authors have no relevant financial or non-financial interests to disclose.

Availability of data and materials

The datasets used and/or analyzed during the current study are available from the corresponding author on reasonable request.

References

1. Ali F, Khan SB, Kamal T, Anwar Y, Alamry KA, Asiri AM (2017) Bactericidal and catalytic performance of green nanocomposite based-on chitosan/carbon black fiber supported monometallic and bimetallic nanoparticles. Chemosphere 188:588–598

2. Ballesteros B, Tobias G, Shao L, Pellicer E, Nogués J, Mendoza E, Green MLH (2008) Steam Purification for the Removal of Graphitic Shells Coating Catalytic Particles and the Shortening of Single-Walled Carbon Nanotubes. Small 4:1501–1506
3. Bian T, Zhang J, Wang Z, Wang Z, Liu L, Meng J, Zhao J, Cai Q, Wang H (2021) MoS2 – induced hollow Cu2O spheres: Synthesis and efficient catalytic performance in the reduction of 4-nitrophenol by NaBH4. Appl Surf Sci 539:148285
4. Bogireddy NKR, Sahare P, Pal U, Méndez SFO, Gomez LM, Agarwal V (2020) Platinum nanoparticle-assembled porous biogenic silica 3D hybrid structures with outstanding 4-nitrophenol degradation performance. Chem Eng J 388:124237
5. Cao H-L, Liu C, Cai F-Y, Qiao X-X, Dichiara AB, Tian C, Lü J (2020) In situ immobilization of ultra-fine Ag NPs onto magnetic Ag@RF@Fe_3O_4 core-satellite nanocomposites for the rapid catalytic reduction of nitrophenols. Water Res 179:115882
6. Cui Y, Ma K, Chen Z, Yang J, Geng Z, Zeng J (2020) Atomic-level insights into strain effect on p-nitrophenol reduction via Au@Pd core–shell nanocubes as an ideal platform. J Catal 381:427–433
7. Duan X, Ning L, Yin Y, Huang Y, Gao J, Lin H, Tan K, Fang H, Ye L, Lu X, Yuan Y (2019) Sulfur Moiety as a Double-Edged Sword for Realizing Ultrafine Supported Metal Nanoclusters with a Cationic Nature. ACS Appl Mater Interfaces 11:11317–11326
8. Ferry A, Schaepe K, Tegeder P, Richter C, Chepiga KM, Ravoo BJ, Glorius F (2015) Negatively Charged N-Heterocyclic Carbene-Stabilized Pd and Au Nanoparticles and Efficient Catalysis in Water. ACS Catal 5:5414–5420
9. Fu Y, Qin L, Huang D, Zeng G, Lai C, Li B, He J, Yi H, Zhang M, Cheng M, Wen X (2019a) Chitosan functionalized activated coke for Au nanoparticles anchoring: Green synthesis and catalytic activities in hydrogenation of nitrophenols and azo dyes. Appl Catal B 255:117740
10. Fu Y, Xu P, Huang D, Zeng G, Lai C, Qin L, Li B, He J, Yi H, Cheng M, Zhang C (2019b) Au nanoparticles decorated on activated coke via a facile preparation for efficient catalytic reduction of nitrophenols and azo dyes. Appl Surf Sci 473:578–588
11. He J, Lai C, Qin L, Li B, Liu S, Jiao L, Fu Y, Huang D, Li L, Zhang M, Liu X, Yi H, Chen L, Li Z (2020) Strategy to improve gold nanoparticles loading efficiency on defect-free high silica ZSM-5 zeolite for the reduction of nitrophenols. Chemosphere 256:127083
12. Jiang B, Zheng J, Lu X, Liu Q, Wu M, Yan Z, Qiu S, Xue Q, Wei Z, Xiao H, Liu M (2013) Degradation of organic dye by pulsed discharge non-thermal plasma technology assisted with modified activated carbon fibers. Chem Eng J 215–216:969–978
13. Jiang S, Wang L, Duan Y, An J, Luo Q, Zhang Y, Tang Y, Huang J, Zhang B, Liu J, Wang D (2021) A novel strategy to construct supported silver nanocomposite as an ultra-high efficient catalyst. Appl Catal B 283:119592
14. Kamal T, Khan SB, Asiri AM (2016) Nickel nanoparticles-chitosan composite coated cellulose filter paper: an efficient and easily recoverable dip-catalyst for pollutants degradation. Environ Pollut 218:625–633
15. Li S, Shu J, Ma S, Yang H, Jin J, Zhang X, Jin R (2021) Engineering three-dimensional nitrogen-doped carbon black embedding nitrogen-doped graphene anchoring ultrafine surface-clean Pd nanoparticles as efficient ethanol oxidation electrocatalyst. Appl Catal B 280:119464
16. Lima IM, Boateng AA, Klasson KT (2010) Physicochemical and adsorptive properties of fast-pyrolysis bio-chars and their steam activated counterparts. Journal of Chemical Technology & Biotechnology 85:1515–1521
17. Lin F-h, Doong R-a (2014) Highly efficient reduction of 4-nitrophenol by heterostructured gold-magnetite nanocatalysts. Appl Catal A 486:32–41
18. Liu X, Wu L, Liu T, Zhang L (2021) In situ confine of Co_3ZnC/Co in N-doped carbon nanotube-grafted graphitic carbon nanoflakes as 1D-2D hierarchical catalysts toward superior redox activity. Appl Catal B 281:119513
19. Neal RD, Hughes RA, Sapkota P, Ptasinska S, Neretina S (2020) Effect of Nanoparticle Ligands on 4-Nitrophenol Reduction: Reaction Rate, Induction Time, and Ligand Desorption. ACS Catal 10:10040–10050
20. Nellaiappan S, Kumar AS, Nisha S, Pillai KC (2017) In-situ preparation of Au (111) oriented nanoparticles trapped carbon nanofiber-chitosan modified electrode for enhanced bifunctional electrocatalysis and sensing of formaldehyde and hydrogen peroxide in neutral pH solution. Electrochim Acta 249:227–240
21. Nguyen TB, Huang C, Doong R-a (2019a) Enhanced catalytic reduction of nitrophenols by sodium borohydride over highly recyclable Au@ graphitic carbon nitride nanocomposites. Appl Catal B 240:337–347
22. Ozerova AM, Komova OV, Mukha SA, Simagina VI, Odegova GV, Arzumanov SS, Bulavchenko OA, Netskina OV (2020) An improved purification of $NaBH_4$ from storage-induced impurities by ammonia assisted crystallization in diglyme. Int J Hydrog Energy 45:30756–30766

23. Qin L, Huang D, Xu P, Zeng G, Lai C, Fu Y, Yi H, Li B, Zhang C, Cheng M, Zhou C, Wen X (2019a) In-situ deposition of gold nanoparticles onto polydopamine-decorated g-C_3N_4 for highly efficient reduction of nitroaromatics in environmental water purification. J Colloid Interface Sci 534:357–369
24. Qin L, Yi H, Zeng G, Lai C, Huang D, Xu P, Fu Y, He J, Li B, Zhang C, Cheng M, Wang H, Liu X (2019b) Hierarchical porous carbon material restricted Au catalyst for highly catalytic reduction of nitroaromatics. J Hazard Mater 380:120864
25. Qin L, Zeng Z, Zeng G, Lai C, Duan A, Xiao R, Huang D, Fu Y, Yi H, Li B, Liu X, Liu S, Zhang M, Jiang D (2019c) Cooperative catalytic performance of bimetallic Ni-Au nanocatalyst for highly efficient hydrogenation of nitroaromatics and corresponding mechanism insight. Appl Catal B 259:118035
26. Qin L, Wang Z, Fu Y, Lai C, Liu X, Li B, Liu S, Yi H, Li L, Zhang M, Li Z, Cao W, Niu Q (2021) Gold nanoparticles-modified $MnFe_2O_4$ with synergistic catalysis for photo-Fenton degradation of tetracycline under neutral pH. J Hazard Mater 414:125448
27. Rajapaksha AU, Vithanage M, Ahmad M, Seo D-C, Cho J-S, Lee S-E, Lee SS, Ok YS (2015) Enhanced sulfamethazine removal by steam-activated invasive plant-derived biochar. J Hazard Mater 290:43–50
28. Reddy SS, Sinha AK, Amarendra G, Shekar NVC, Bhalerao GM (2020) Enhancement of graphitic order in carbon black using precursor additive. Diam Relat Mater 101:107539
29. Revathy TA, Dhanavel S, Sivaranjani T, Narayanan V, Maiyalagan T, Stephen A (2018) Highly active graphene-supported palladium-nickel alloy nanoparticles for catalytic reduction of 4-nitrophenol. Appl Surf Sci 449:764–771
30. Shcherban ND, Yaremov PS, Ilyin VG, Ovcharova MV (2014) Influence of the method of activation on the structural and sorption properties of the products of carbonization of sucrose. J Anal Appl Pyrol 107:155–164
31. Shin KS, Cho YK, Choi J-Y, Kim K (2012) Facile synthesis of silver-deposited silanized magnetite nanoparticles and their application for catalytic reduction of nitrophenols. Appl Catal A 413:170–175
32. Song J, Xu L, Xing R, Li Q, Zhou C, Liu D, Song H (2014) : Synthesis of Au/Graphene Oxide Composites for Selective and Sensitive Electrochemical Detection of Ascorbic Acid. Scientific Reports 4
33. Tan L, Tan B (2020) Functionalized hierarchical porous polymeric monoliths as versatile platforms to support uniform and ultrafine metal nanoparticles for heterogeneous catalysis. Chem Eng J 390:124485
34. Wang M-x, Xu F, Liu Q, Sun H-f, Cheng R-h, He H, Stach EA, Xie J (2011) Enhancing the catalytic performance of Pt/C catalysts using steam-etched carbon blacks as a catalyst support. Carbon 49:256–265
35. Wang R-Z, Huang D-L, Liu Y-G, Zhang C, Lai C, Wang X, Zeng G-M, Zhang Q, Gong X-M, Xu P (2020) Synergistic removal of copper and tetracycline from aqueous solution by steam-activated bamboo-derived biochar. J Hazard Mater 384:121470
36. Wang Y-L, Dai Y-M, Tsai M-H (2021) Highly efficient and recyclable Fe_3C/Au@NG catalyst for 4-nitrophenol reduction. Catal Commun 149:106251
37. Xia J, He G, Zhang L, Sun X, Wang X (2016) Hydrogenation of nitrophenols catalyzed by carbon black-supported nickel nanoparticles under mild conditions. Appl Catal B 180:408–415
38. Zhang M, Su X, Ma L, Khan A, Wang L, Wang J, Maloletnev AS, Yang C (2021) Promotion effects of halloysite nanotubes on catalytic activity of Co_3O_4 nanoparticles toward reduction of 4-nitrophenol and organic dyes. J Hazard Mater 403:123870
39. Zhang Q-P, Sun Y-l, Cheng G, Wang Z, Ma H, Ding S-Y, Tan B, Bu J-h, Zhang C (2020) Highly dispersed gold nanoparticles anchoring on post-modified covalent organic framework for catalytic application. Chem Eng J 391:123471
40. Zhao N, He C, Jiang Z, Li J, Li Y (2007) Physical activation and characterization of multi-walled carbon nanotubes catalytically synthesized from methane. Mater Lett 61:681–685

Figures

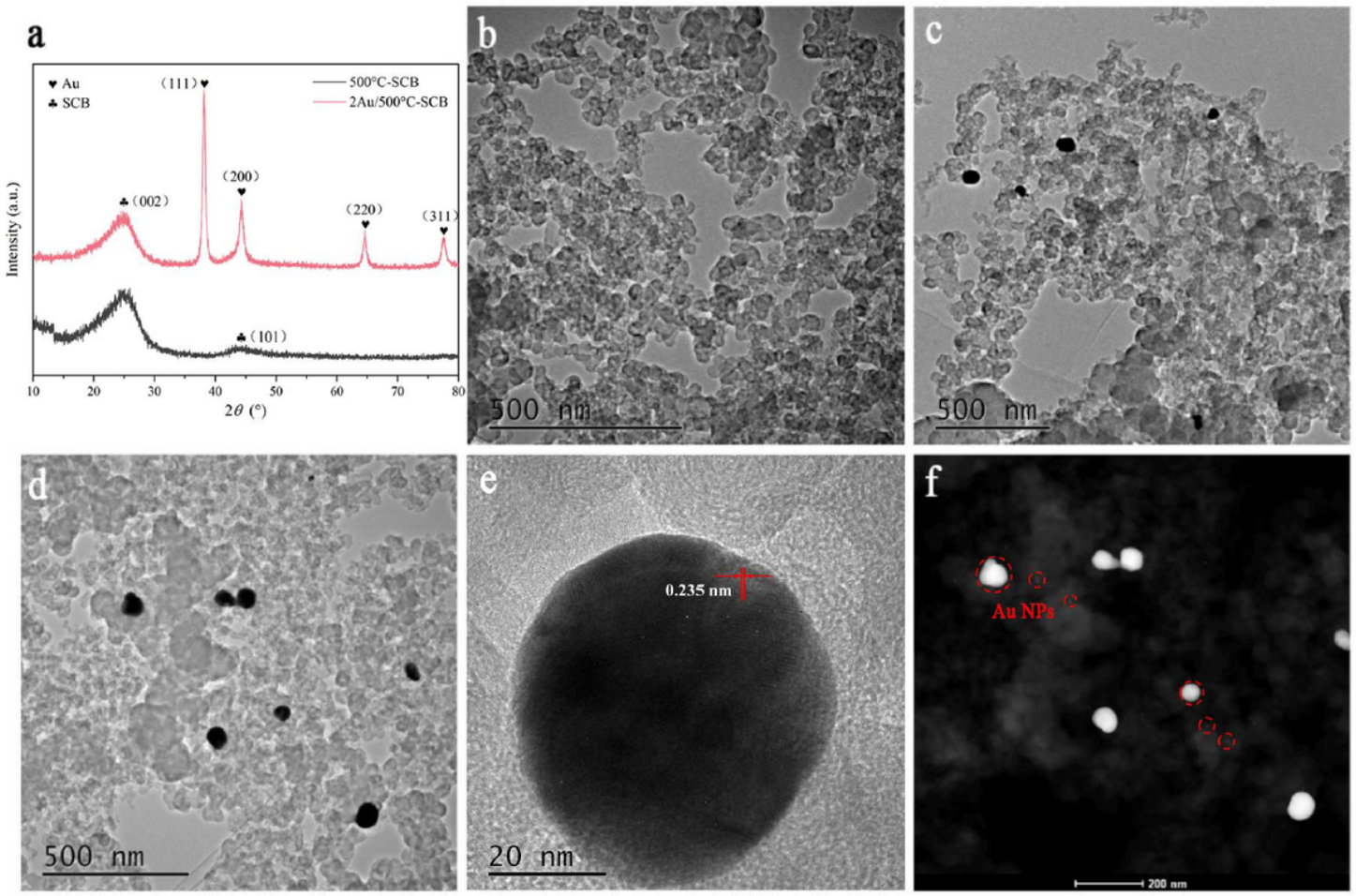

Figure 1

1 (a) X-ray diffraction spectra of 500°C-SCB and 2Au/500°C-SCB, TEM and HRTEM of (b) 500°C-SCB and (c-e) 2Au/500°C-SCB, (f) STEM image of 2Au/500°C-SCB.

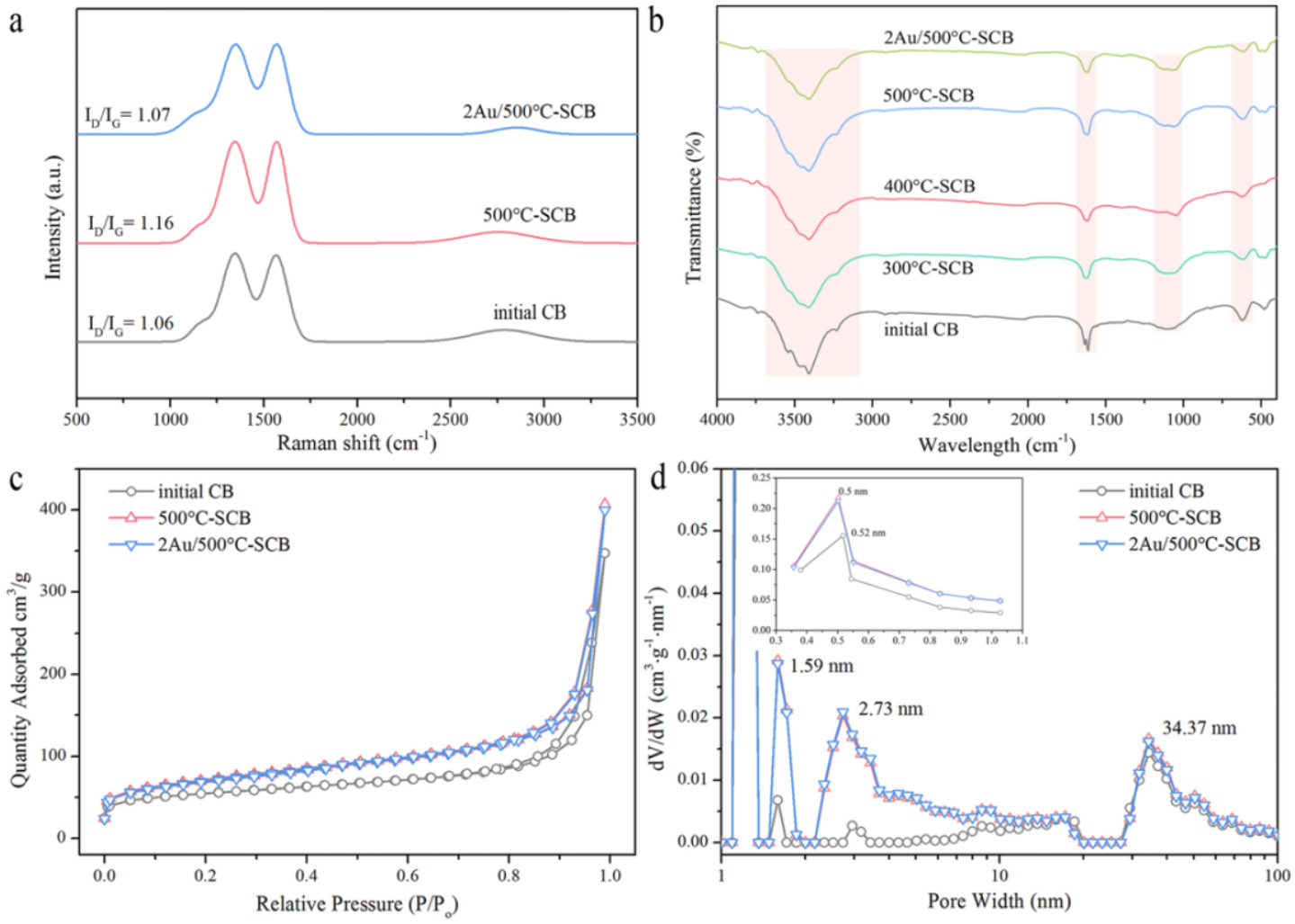

Figure 2

(a) Raman spectra of initial CB, 500°C-SCB and 2Au/500°C-SCB, (b) FT-IR spectra of 300°C-SCB, 400°C-SCB, 500°C-SCB, and 2Au/500°C-SCB. (c) N_2 adsorption-desorption isotherms and (d) pore size distribution of initial CB, 500°C-SCB and 2Au/500°C-SCB.

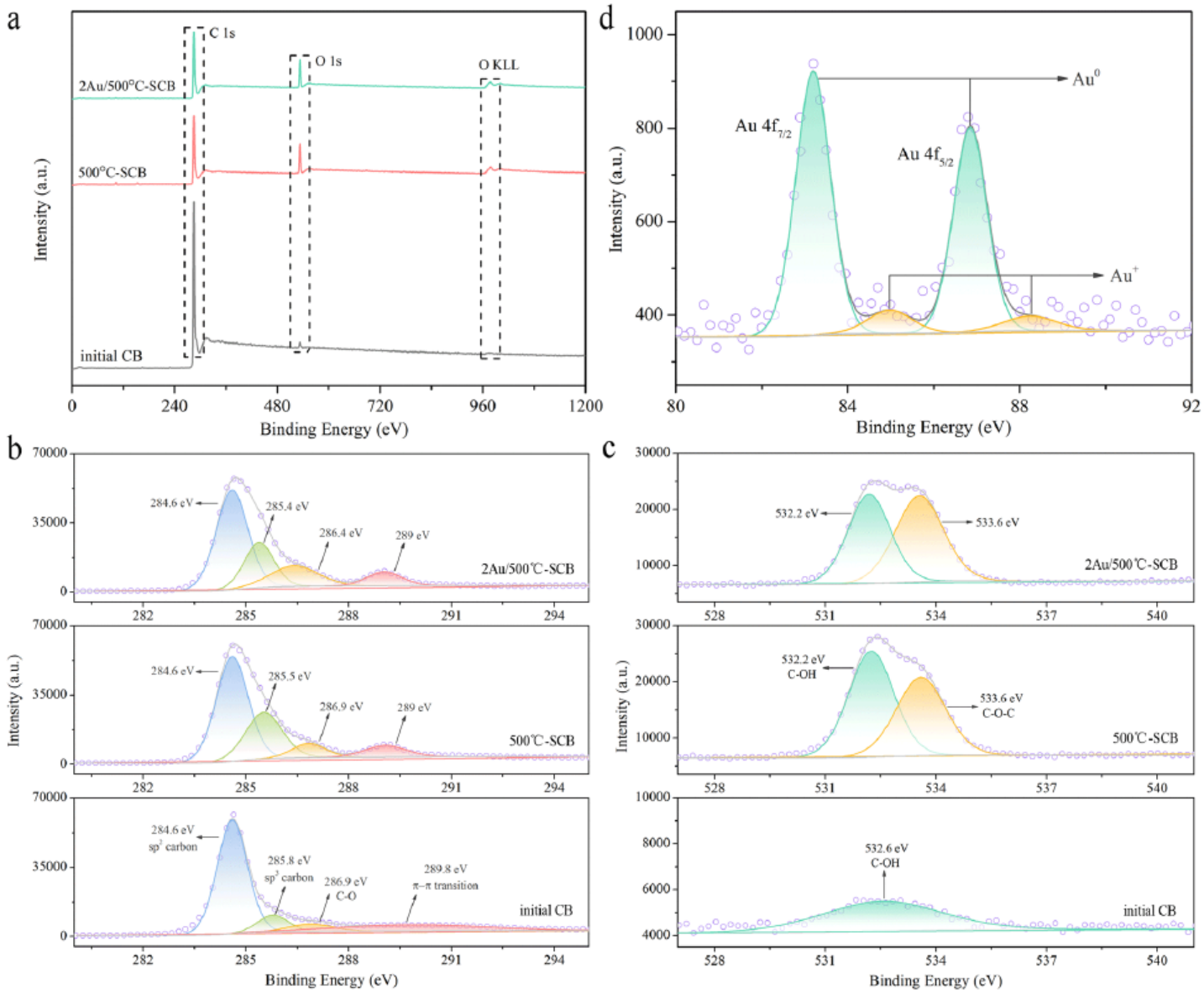

Figure 3

(a) Full XPS spectra, high-resolution XPS spectra of (b) C 1s, (c) O 1s, and (d) Au 4f of initial CB, 500°C-SCB, and 2Au/500°C-SCB.

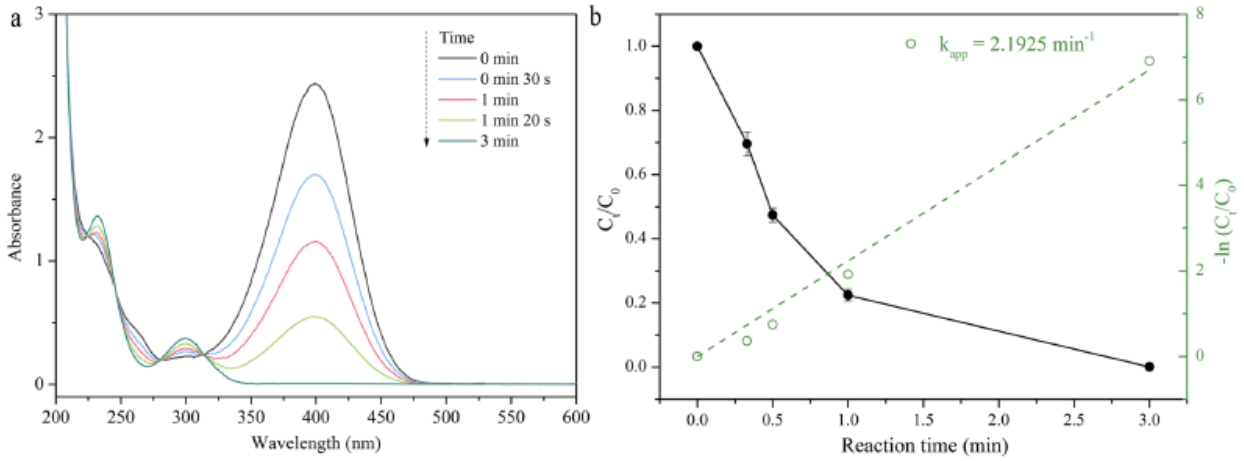

Figure 4

(a) Time-dependent UV-Vis absorption spectra of 4-NP reduction over 2Au/500°C-SCB, and (b) plots of C_t/C_0 and -ln (C_t/C_0) *vs.* time. Reaction conditions: C(4-NP) = 0.2 mM, C($NaBH_4$) = 40 mM, m(2Au/500°C-SCB) = 10 mg, initial pH = 5.62, and room temperature.

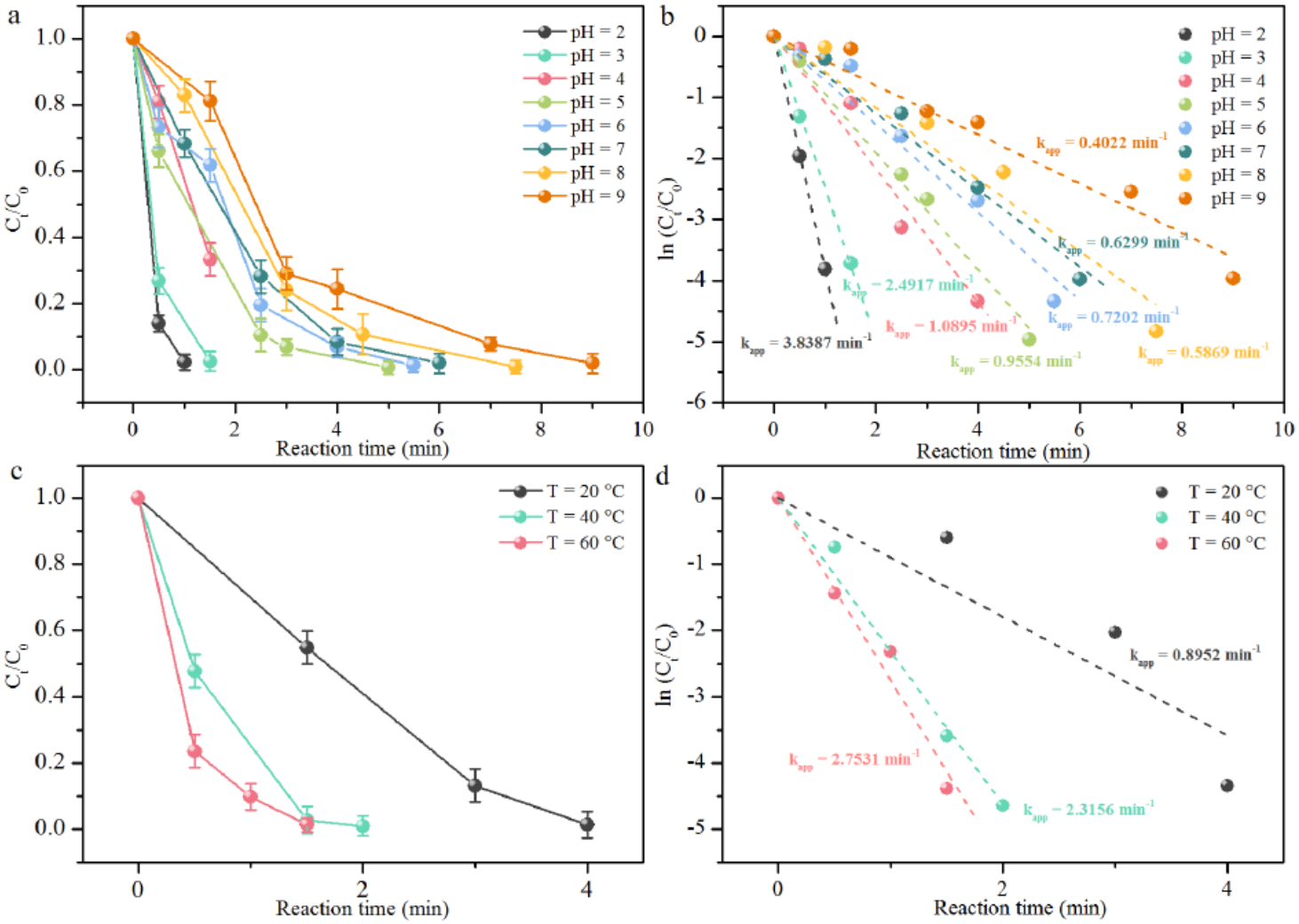

Figure 5

(a) Plots of C_t/C_0 and (b) -ln (C_t/C_0) *vs.* reaction time of 4-NP reduction under different pH conditions. (c) Plots of C_t/C_0 and (d) -ln (C_t/C_0) *vs.* reaction time of 4-NP reduction under different reaction temperature (T = 20°C, 40°C, and 60°C) over 2Au/500°C-SCB catalysts. Reaction conditions: C(4-NP) = 0.2 mM, C($NaBH_4$) = 40 mM, m(2Au/500°C-SCB) = 10 mg.

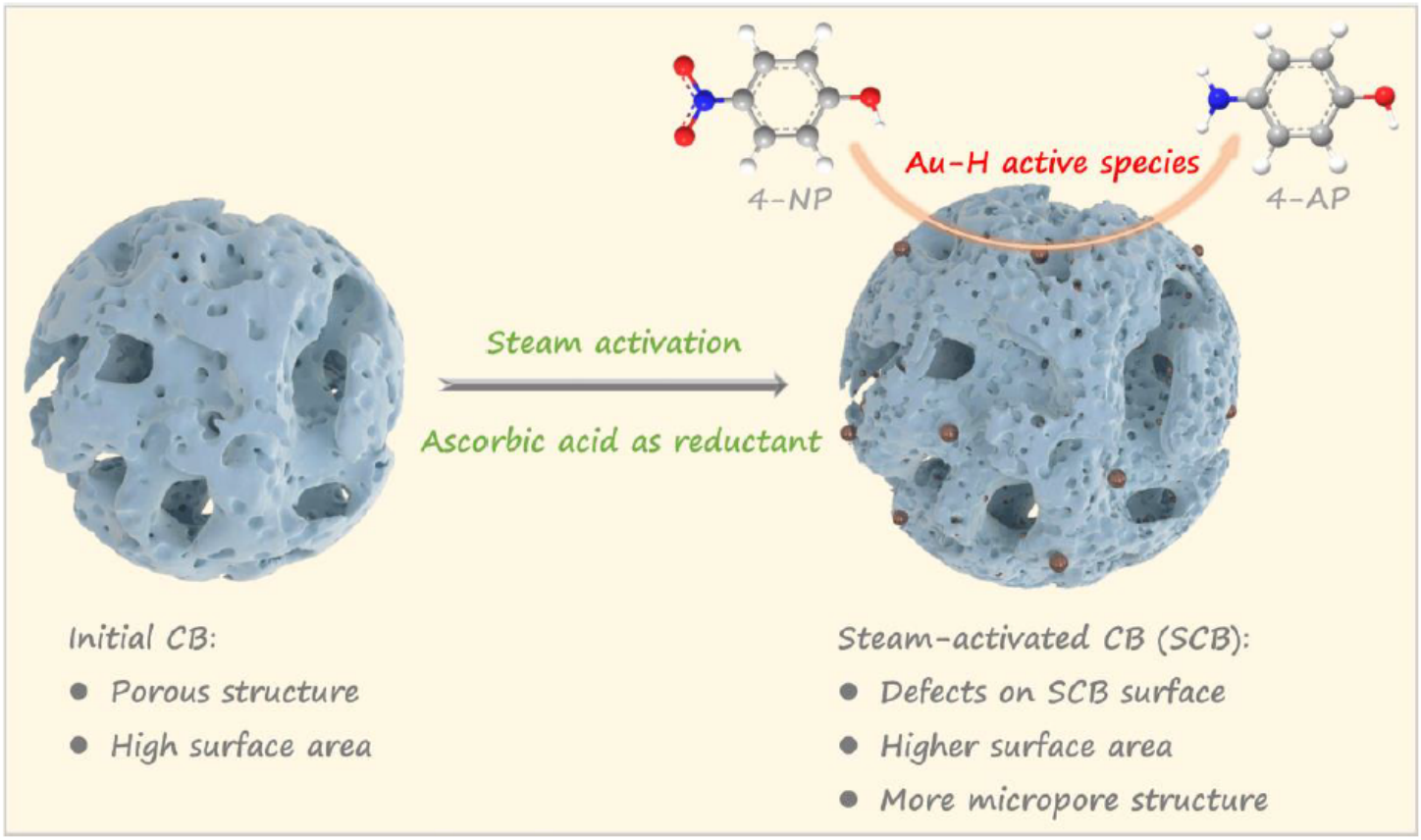

Figure 6

Schematic representation of the green and simple method for preparing 2Au/500°C-SCB catalysts used for reduction of 4-NP.

Supplementary Files

This is a list of supplementary files associated with this preprint. Click to download.

- Supportinginformation.docx